Modelling wind driven airflow rate with CFD and verification of approximation formulas based on wind pressure coefficients

S. Leenknegt[1]*, B. Piret[1], A. Tablada de la Torre[1], D. Saelens[1]

[(1)] Division of Building Physics, Department of Civil Engineering, K.U.Leuven, Leuven, Belgium

* contact information: sarah.leenknegt@bwk.kuleuven.be

ABSTRACT

An isothermal CFD study was made of a building perpendicular to the wind direction. The building was modelled with a closed façade, and consecutively with one and multiple openings. The sensitivity was investigated for different turbulence models, meshes and near wall treatments, both in 2D and 3D. A large sensitivity was found to the modelling options with regard to the predicted wind pressure coefficients (C_p) distribution, but less with regard to the predicted flow rate through the openings. The distribution of C_p was compared to literature and the influence of the openings on the wind pressure coefficients is investigated. Openings have a large influence on local C_p on the windward side, but only limited on the leeward side. The simulated airflow rates were recalculated using theoretical approximation formulas. The calculated values showed better agreement to the CFD-simulations when the C_p in front of the openings were used, compared the C_p taken at a closed wall.

KEYWORDS

Wind-driven ventilation, CFD, internal airflow, night ventilation

1 Introduction

Night ventilation is a method to cool a building by using the thermal inertia of walls and floors to buffer the heat during day. Wind, thermal buoyancy or fans can be used to achieve the necessary high air change rates during night time to cool down the exposed surfaces [1]. In order to minimize the energy use, ideally, this process is driven by natural driving forces. However, a large uncertainty in the realizable cooling potential is in the prediction of natural ventilation flows [2], [3]. The focus of this paper is on the prediction of wind-driven airflow rates with Computational Fluid Dynamics (CFD) versus approximation formulas from literature. Commonly, a network model is assumed, where the flow rate is predicted based on wind pressure coefficients, combined with a discharge coefficient for the opening to take into account friction losses. In this paper, it is investigated how these wind pressures vary at the location of the openings, and how this influences the predicted flow rate. A rectangular opening is used, with wind direction perpendicular to the opening.

2 Methodology

The object of the study is a building of 25 m high, 20 m wide and 30 m long, which is modelled with CFD (Fluent 6.3 and Fluent 12 (ANSYS)). In a first step, a validation is made for a scaled model of the building (1/200), using wind tunnel measurements from the CEDVAL[1] database provided by the Meteorological Institute of the Technical University in Hamburg [4]. Secondly, the scaled model is rescaled to full scale to determine the wind pressure on the façades. Consequently, one, and later multiple, openings are incorporated in the building, resulting in a modified distribution of the wind pressure coefficient on the façade and air flowing through the opening(s). An illustration is given in Fig. 1.

[1] CEDVAL = Compilation of experimental data for validation of micro-scale dispersion models

First an investigation is made of the sensitivity with regard to the following modelling options. Turbulence modelling is investigated through the following RANS models: realizable k-ε and SST k-ω. Near wall modelling is investigated through standard wall functions, non equilibrium wall functions and enhanced wall treatment. Finally, mesh independency is investigated.

Secondly, a discussion is made on the distribution of the wind pressure coefficients on the facade and the profile at the openings. Also, a discussion is made of the airflow rate, predicted by the simulations and calculated with approximation formulas.

3 Modelling

There are a number of specific challenges to the modelling of wind flow around buildings with CFD [5],[6]. This will not be discussed in detail here; rather the choices made for this research will be recounted. The simulation is isothermal: buoyancy is not taken into account.

3.1 Boundary conditions

The wind velocity at the inlet of the flow domain will vary with the height, as it is located in the lower part of the atmospheric boundary layer (ABL). To use the data from CEDVAL [4] for validation, the velocity profile at the inlet must correspond to the inlet at the wind tunnel, which was achieved with a power law given in equation (1) (scaled model), where *U(y)* is the profile of the x-velocity over the height (m/s), U_{ref} is the reference x-velocity at reference height h_{ref} (m) and α describes the type of environment upstream from the inlet. The turbulent kinetic energy k and the turbulent dissipation rate ε at the inlet are given by equations (2) and (4).

Vertical x-velocity profile $$U(y) = U_{ref}\left(\frac{y}{h_{ref}}\right)^{\alpha} = 6 \cdot \left(\frac{y}{0.5}\right)^{0.22} \quad (1)$$

Turbulent kinetic energy $$k(y) = 1.5 \cdot I(y)^2 \cdot U(y)^2 \quad [7] \quad (2)$$

Turbulence intensity $$I(y) = 0.05 + 0.18 \cdot \exp(-0.08u) \quad (3)$$

Turbulent dissipation rate $$\varepsilon(y) = \frac{(u^*)^3}{\kappa(y + y_0)} = \frac{0.377^3}{0.42(y + 7 \cdot 10^{-4})} \quad (4)$$

Friction velocity $$u^*_{ABL} = \frac{U(y_{ref})\kappa}{ln\left(\frac{y_{ref} + y_0}{y_0}\right)} \quad (5)$$

3.2 Roughness

A common problem in CFD wind studies is to simulate a correct progression of the velocity profile over the upstream part of the domain, that is from the inlet towards the area of interest. In reality, this is determined by the roughness of the terrain y_0, while the software package Fluent uses an equivalent sand-grain roughness K_s in the wall functions for the near wall modelling.

For this research, the recommendations from [5] and [8] were followed for the value of K_s. The boundary conditions used in the simulation of the model are summarized in Table 1.

3.3 Mesh and turbulence model

This CFD-study concern two types of flow: free flow around an obstacle and wall bounded flow. For flow in an enclosed environment, [9] gives following conclusions with regard to the most common RANS models. Both standard and RNG k-ε models provide reasonable results, if no special situations occur (e.g. strong buoyancy). The SST k-ω model gives even better results, but still requires further validation.

For wind studies, commonly applied RANS models are the standard k-ε model for its good stability, with as alternatives the realizable or RNG k-ε [8]. As there are no fixed guidelines to the selection of a turbulence model, [8] recommends to perform a sensitivity study and to compare the results to measurement data, relevant to the specific case.

A sensitivity study is made with regard to turbulence models, near-wall treatment and mesh size.

- For the validation study with the scaled building model, five meshes were investigated, as well as four combinations of turbulence model and near-wall modelling; see also respectively Table 2 and Table 3.
- For the 2D full scale study (closed and open), the realizable k-ε (non-equilibrium and standard wall functions) and SST k-ω model were applied, together with the base mesh from the validation (me3) and an extra mesh (mehi) with refinement on all edges by approximately a factor 2.
- Finally, for the 3D study of the open building (one and multiple openings) the realizable k-ε model with standard wall functions was investigated with a base mesh (me3) and a refined mesh (mehi). The SST k-ω was tested only with the base mesh (me3) and one opening. It was also investigated if the calculation domain could be halved by introducing a symmetry plane. As all boundary conditions are symmetric, this is a justified simplification.

In the following paragraph, an overview is given of the validation of the scaled closed building model. The validation is done by comparing x-velocities of the flow throughout the flow domain. The experimental data from CEDVAL only contain velocity profiles, therefore the resulting wind pressure coefficients are verified by using the TNO C_p-Generator [10], which is a database of C_p-coefficients based on systematic wind tunnel experiments and various studies with several validations [11],[12].

3.4 Scaled closed building: validation of velocity profiles

The validation study on the scaled building block is described in detail in [13], and was made using the recommendations of [8]. Generally, the difference between the experimental and simulation data is larger than the difference within the simulation results. The main difference

between measurement and simulation is situated at the leeward vortex (behind the building) and the roof, where Fluent predicts leeward vortices that are both too high and longer than in the wind tunnel. Furthermore, there is only limited difference between the different wall treatments of the realizable k-ε model. The k-ε model also performs slightly better than the k-ω model in the prediction of the velocity throughout the flow domain and is more stable.

Finally, also a mesh dependency study was performed with 5 meshes (see Table 2). As the results were relatively independent of the mesh, the resolution of the base mesh (me3) is sufficient to predict to velocities around the closed building.

4 Discussion of results

4.1 Full scale closed building

After the validation of the scaled model, all the dimensions of the small scale building are multiplied by a factor 200 (25/20/30 m). The velocity profile from equation (1) is rescaled by increasing the reference height h_{ref} from 0.5 to 100 m, while α and U_{ref} are unchanged. Consequently, also the k - and ε - profile is resized. There is good correspondence between the velocity profiles for the scaled and full-scale building. However, there are significant differences between the C_p-values, both between scaled and full scale model as between 2D and 3D simulation, which is illustrated in Fig. 2. The values plotted here are taken from the vertical centre line just next to the wall surface, starting at the ground on the windward side, continuing over the windward side, the roof and the leeward side. The TNO C_p-Generator gives higher negative values on the roof and on the leeward side as well as a much higher peak at the windward side of the roof. The full scale model agrees better with the results from the TNO C_p-Generator on the windward side and the roof, but shows still lower values on the leeward side. This indicates that a full scale study is indeed necessary in order to make conclusions.

4.2 Full scale open building: global C_p profile over facade

Fig. 3 shows the C_p-values in the case of one opening, with a comparison of the realizable k-ε model with standard wall functions (ke-stw) and the SST k-ω model (kw). The results from 2D and 3D are compared as well. For reference, the values from the TNO C_p-Generator for a closed building are included. A decrease in the local pressure coefficients is visible at the opening on the windward side. At the leeward side, a shift is visible as well, though less pronounced. A comparison of the base mesh (me3) and the refined mesh (mehi) showed that the base mesh is sufficient.

With regard to the modelling sensitivity, following remarks are made for the case with one opening (Fig. 3):

- **2D versus 3D**: the 2D simulations overestimate the leeward pressure coefficients, as was already mentioned before but is visualised here. Also at the windward side, the correspondence of the 3D-results to the TNO C_p-Generator is better (zone close to roof). This shows that a 3D simulation is required.
- **Turbulence model**: The SST k-ω model gives an unrealistic profile of the under pressure at the roof. Also at windward facade, the values are significantly lower, but at leeward facade, there is a large similarity with the realizable k-ε model.

Fig. 4 shows a similar comparison for the case with multiple (mult) openings. Remarkable is the large influence of the openings on the windward side and the very limited influence on the leeward side. For this case, a comparison was also made between a flow domain with and without symmetry plane, showing that this does not alter the results for this wind direction.

Fig. 5 gives a compilation of the previous three figures. The overall wind pressure coefficient between the openings on the windward side is slightly higher for the case with multiple openings

compared to the case with one opening. For all openings, the local pressure drop at the windward side is in the same order of magnitude, for the central opening for example from 0.6 to 0.4.

4.3 Full scale open building: local C_p and velocities at the openings

Fig. 6 and Fig. 7 show respectively the C_p- and x-velocity-profile over the opening: (a) shows the opening at the windward side while (b) shows the opening at the leeward side. Results are given for the internal zone (middle of the building) for the case with one and multiple (mult) openings. Following comparisons are shown in these figures:

- 2D versus 3D
- one versus multiple openings
- the realizable k-ε model with either standard wall functions (ke-stw) or non-equilibrium wall functions (ke-ne) and the SST k-ω model (kw)
- the base mesh (me3), the refined mesh (mehi) and the mesh with symmetry plane (h-)

The C_p-values at the windward side, shown in Fig. 6-a, show good agreement between 2D and 3D. At the leeward side however in Fig. 6-b, the C_p have very large differences between 2D and 3D which is consistent with the previous results.

For the velocities at the windward side (Fig. 7-a) a clear difference is seen between 2D and 3D simulations, but the different turbulence models perform similar (compare 3D_one_ke-stw and 3D_one_kw). For the velocities at the leeward side (Fig. 7-b), there is a large spread over all the displayed results. We see here that there is a large sensitivity to the different turbulence models (compare 3D_one_ke-stw and 3D_one_kw).

The influence of one compared to multiple openings is limited (Fig. 7-b: compare 3D_one_ke-stw and 3D_mult_ke-stw). This indicates that the wind-driven flow through one opening will

have a limited influence from the presence of other openings, and may be investigated individually. This must be verified with further simulations and different opening locations, but could simplify the geometric model significantly.

5 Prediction of airflow rate

5.1 Results from the CFD-study

The airflow rates as predicted by the CFD-simulations are compared in Table 4. The flow rates in the 2D simulation represent an overestimation, as they assume an infinite opening length and ignore the additional friction losses at the vertical opening boundaries. An imbalance between incoming and outgoing flow was observed, which is most likely due to an insufficiently fine mesh at the openings. It is clear that even in the CFD-study, there is uncertainty on the predicted mass flows, but the differences between the 3D-results are limited to maximum +/- 5%.

5.2 Theoretical calculation of airflow rate

Wind-driven flow rates can be estimated with approximation formulas (resistance model), which use the wind pressure in combination with the opening characteristics. Therefore, the discharge coefficient C_d, which is an empirical correction factor to indicate the "flow efficiency" of an opening, is determined for this specific case. Typically, a value of 0.6-0.65 is assumed for rectangular openings, though it is shown that C_d is not a constant [14],[15]. C_d is defined by the so-called orifice equation, given by equation (6).

$$C_d = \frac{G_a}{A \cdot \sqrt{\frac{2\Delta P}{\rho_0}}} \qquad (6)$$

and here:

$\Delta P_{in} = |P_{front} - P_{int}|$

$\Delta P_{out} = |P_{back} - P_{int}|$

G_a [m³/s]

Special care should be taken in the determination of the pressure difference ΔP over the opening. ΔP is well defined in pipe flows, but not straightforward for flow through wall openings [16]. For this comparison, it is particularly important that the same pressure differences are later also

applied in the approximation formulas. Here, the pressure difference was taken between the area weighted average static pressure at 20 cm outside the inlet/outlet opening and an internal static pressure P_{int}, which is defined here as the area weighted average of the static pressure in a vertical cross section through the middle of the internal zone.

Table 5 gives an overview of area weighted average values for both 2D and 3D simulations of following parameters: P_{int}, P_1, P_2, ΔP, C_p and the resulting C_d for each opening. Notice that the C_p have a v_{ref} of 6 m/s and were also taken at 20 cm distance from façade and opening.

In a second step, the airflow can be recalculated theoretically for each simulation, using the C_p-values from Table 5. As the simulations are isothermal, pressure differences due to thermal stack are neglected. Two methods are used. The first one is the method of Aynsley [16], which is a simplified empirical method, giving the flow for cross ventilation by equation (7). A second method gives an iterative approach, described by Liddament (2009) [17], where the pressure outside both openings is determined by equation (8). Next, the conservation of mass in equation (9) is iterated for the *j (= 2)* openings, until p_{int} is determined. Both methods use the same basic equations, and should therefore give the same results.

$$Q = \rho \cdot v_{ref} \cdot \sqrt{\frac{C_{p,front} - C_{p,back}}{\frac{1}{A_{front}^2 C_{d,front}^2} + \frac{1}{A_{back}^2 C_{d,back}^2}}} \quad \text{[kg/s]} \quad (7)$$

$$p_{w,front/back} = 0.5 \cdot C_{p,front/back} \cdot \rho \cdot v_{ref}^2 \quad \text{[Pa]} \quad (8)$$

$$\sum_{i=1}^{j} \rho_i \cdot C_{d,i} \cdot A_i \cdot \sqrt{\frac{2}{\rho_i}} \cdot \left|p_{w,i} - p_{int}\right|^{n_i} \left[\frac{p_{w,i} - p_{int}}{\left|p_{w,i} - p_{int}\right|}\right] = 0 \quad (9)$$

The results are given in Fig. 8: in (a) default values are assumed for C_d (0.65 for a rectangular opening) and n_i (0.5 for turbulent flow), while (b) shows the results when C_d from the simulations were used. The vertical axis indicates which simulation was used as a reference. The 2D-results are omitted in (b), as C_d can only be determined from a 3D simulation. The results of Aynsley and Liddament are indeed identical.

On Fig. 8-a, there is 9 to 18% difference between the calculated and the simulated flow rate over all the 3D simulations. When the calculated C_d-values are applied in Fig. 8-b, the calculated mass flow rates are nearly identical (difference between 2 to 5%) to the simulations. Notice that for these simplified formulas, the C_p values just in front of the openings were used, though they are usually applied with C_p-values on the closed facade. When comparing to the results with the C_p-values from the closed case (3D_cl_ke-ne_me3), there is a difference of 9 to 11% compared to the 3D CFD-results.

6 Conclusions

Wind-driven ventilation rates are predicted using wind pressure coefficients and the characteristics of the opening. In this paper, a CFD-wind study was made of a building with closed facade, and one and later multiple openings. The sensitivity study showed that the wind pressure must be simulated in a full scale 3D model and that there were large differences between the realizable k-ε and SST k-ω model with regard to the C_p on the windward side and roof. The first model showed better agreement with values from literature. The predicted flow rates were less sensitive to the turbulence model.

The openings in the building cause a local reduction of the C_p in the order of 0.2 on the windward side. In case of multiple openings, the influence on C_p-profile on the leeward side was

limited. The local velocity and C_p profile at the openings showed only small influence from the presence of adjacent openings.

The airflow rate through the opening was recalculated with approximation formulas by Aynsley and Liddament. Only 2 to 5% difference was seen between simulated and calculated flow rates when the applied C_p*'s* were taken next to the opening and the applied C_d was deduced from the simulation results.

ACKNOWLEDGEMENTS

This research was funded by the Research Foundation Flanders (FWO Vlaanderen). Their financial contribution is greatly appreciated.

REFERENCES

[1] Artmann, N. (2009), PhD-thesis, *Cooling of the building structure by night-time ventilation*, Aalborg University, Denmark.

[2] Breesch, H. (2006), PhD-thesis, *Night ventilation: uncertainty and sensitivity analysis*, UGent, Belgium.

[3] Artmann et al. (2008), *Parameter study on performance of building cooling by night-time ventilation*, Renewable Energy 33 (12), p. 2589-2598.

[4] University of Hamburg, Meteorological Institute, Compilation of experimental data for validation of microscale dispersion models (CEDVAL).

[5] Blocken et al. (2007), *CFD simulation of the atmospheric boundary layer: wall function problems*, Atmospheric Environment 41, p. 238-252.

[6] Saathoff et al. (1995), *Effects of model scale in estimating pollutant dispersion near buildings*, Journal of Wind Engineering and Industrial Aerodynamics, Vol. 54-55, p 549-559.

[7] Blocken, B., Persoon, J. (2009), *Pedestrian wind comfort around a large football stadium in an urban environment: CFD simulation, validation and application of the new Dutch wind nuisance standard*, Journal of Wind Engineering and Industrial Aerodynamics, Vol. 97, nr. 5-6, p. 255-270.

[8] Franke et al. (2007), *Best practice guideline for the CFD simulation of flows in urban environment*, COST Action 732 – Quality assurance and improvements of microscale meteorological models, 2007.

[9] Zhai et al. (2007), *Evaluation of various turbulence models in predicting airflow and turbulence in enclosed environments by CFD: Part 1: Summary of prevalent turbulence models*, HVAC&R Research 13(6).

[10] TNO Building and Construction Research, TNO Web Application C_p-Generator.

[11] IEA – ECBCS, Annex 35: HybVent (2003).

[12] de Wit, M.S. (1999), *Uncertainty in wind pressure coefficients for low-rise buildings*, Delft University of Technology.

[13] Piret, B. (2009), *CFD-simulation of wind-driven night ventilation in office buildings*, Master Thesis, K.U.Leuven, Leuven, Belgium.

[14] Heiselberg et al. (2001), *Characteristics of airflow from open windows*, Building and Environment, Vol. 36, nr. 7, p. 859-869.

[15] Chu et al. (2009), *Turbulence effects on the discharge coefficient and mean flow rate of wind-driven cross-ventilation*, Building and Environment, nr. 44, p. 2064-2072.

[16] Aynsley, R.M. (1997), *A resistance approach to analysis of natural ventilation airflow networks*, Journal of Wind Engineering and Industrial Aerodynamics, nr. 67-68, p. 711-719.

[17] Liddament, M. (2009), VEETECH Ltd. - Online Tutorials.

Tables

Table 1: Boundary conditions for CFD-simulation of the model (y_0 in the wind tunnel is 0.7 mm, for the full scale building y_0 is 0.14 m)

Faces	**Boundary**	**Parameters**		
Ground	WALL	$K_{s,scaled}$ = 0.0086 m	$K_{s,full}$ = 1.74 m	C_s = 0.8
Building	WALL	$K_{s,scaled}$ = 0 m	$K_{s,full}$ = 0 m	C_s = 0.5
Left side	SYMMETRY	$K_{s,scaled}$ = 0 m	$K_{s,full}$ = 0 m	C_s = 0.5
Right side	SYMMETRY	$K_{s,scaled}$ = 0 m	$K_{s,full}$ = 0 m	C_s = 0.5
Sky	SYMMETRY	$K_{s,scaled}$ = 0 m	$K_{s,full}$ = 0 m	C_s = 0.5
Inlet	VELOCITY INLET	U(y)	equation (1)	input profile
		k(y)	equation (2)	input profile
		ε(y)	equation (4)	input profile
Outlet	PRESSURE OUTLET	p_{gauge} = 0 Pa		
		k(y)	equation (2)	input profile
		ε(y)	equation (4)	input profile

Table 2: Mesh sensitivity analysis, applied to CFD-model of scaled wind tunnel building block

mesh 3	base mesh (me3)	20 $.10^4$ cells
mesh 1	2x more cells/edge	160.10^4 cells
mesh 2	√2x more cells/edge	51 $.10^4$ cells
mesh 4	√2x less cells/edge	14 $.10^4$ cells
mesh 5	2x less cells/edge	2 $.10^4$ cells

Table 3: Model sensitivity

Model	Turbulence model	Near wall modelling
1	Realizable k-ε	enhanced wall functions with pressure gradient
2		non-equilibrium wall functions
3		standard wall functions
4	Standard k-ω	shear flow corrections (SST)

Table 4: Comparison of wind-driven ventilation according to CFD-results: velocity and mass flow

	2D						**3D**				
# OP.	**ONE**			**MULT.**			**ONE**		**MULT.**		
	ke-ne	**ke-stw**	**kw**	**ke-ne**	**ke-stw**	**kw**	**ke-stw_h**	**kw_h**	**ke-stw_h**	**ke-stw**	
$\mathbf{v_{x,in}}$	2.98	2.96	2.84	2.92	2.90	3.11	2.27	2.25	2.27	2.22	**m/s**
$\mathbf{v_{x,out}}$	2.75	2.77	2.69	2.72	2.70	2.84	2.18	2.20	2.18	2.22	**m/s**
$\mathbf{m_{in}}$	9.117	9.070	8.693	8.946	8.874	9.522	6.941	6.89	6.937	6.811	**kg/s**
$\mathbf{m_{out}}$	8.432	8.480	8.240	8.329	8.255	8.713	6.687	6.74	6.690	6.812	**kg/s**

Table 5: Comparison of wind-driven ventilation according to 3D CFD-results: boundary conditions at the opening

# openings	**ONE**		**MULT.**		
case	**ke-stw_h-mehi**	**kw_h-me3**	**ke-stw_h-mehi**	**ke-stw_mehi**	**units**
$\mathbf{P_{int}}$	1.35	2.81	0.98	1.93	**Pa**
$\mathbf{P_{front}}$	8.07	7.56	9.13	7.95	**Pa**
$\mathbf{P_{back}}$	-3.76	-2.61	-3.33	-4.26	**Pa**
$\mathbf{\Delta P_{in}}$	6.72	4.75	8.15	6.02	**Pa**
$\mathbf{\Delta P_{out}}$	5.11	5.42	4.32	6.19	**Pa**
$\mathbf{C_{p,f}}$	0.37	0.34	0.36	0.41	-
$\mathbf{C_{p,b}}$	-0.17	-0.12	-0.19	-0.15	-
$\mathbf{C_{d,in}}$	0.68	0.81	0.62	0.71	-
$\mathbf{C_{d,out}}$	0.76	0.74	0.82	0.70	-

Figures

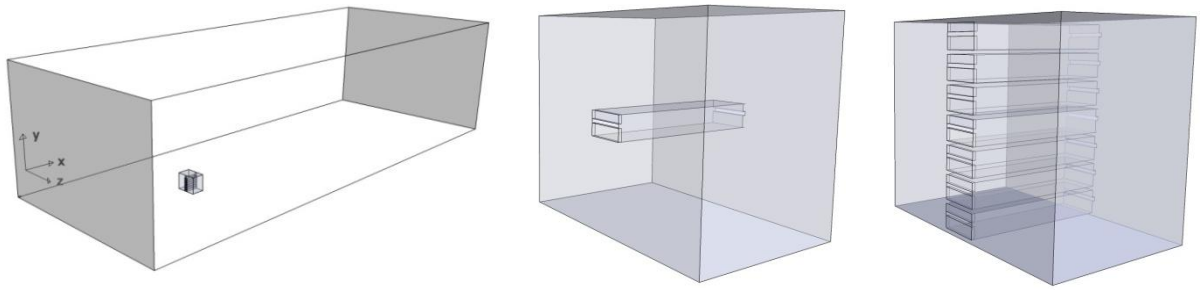

(a) (b) (c)

Fig. 1. Overview of (a) building in flow domain and 3D model of the building with (b) one and (c) multiple openings

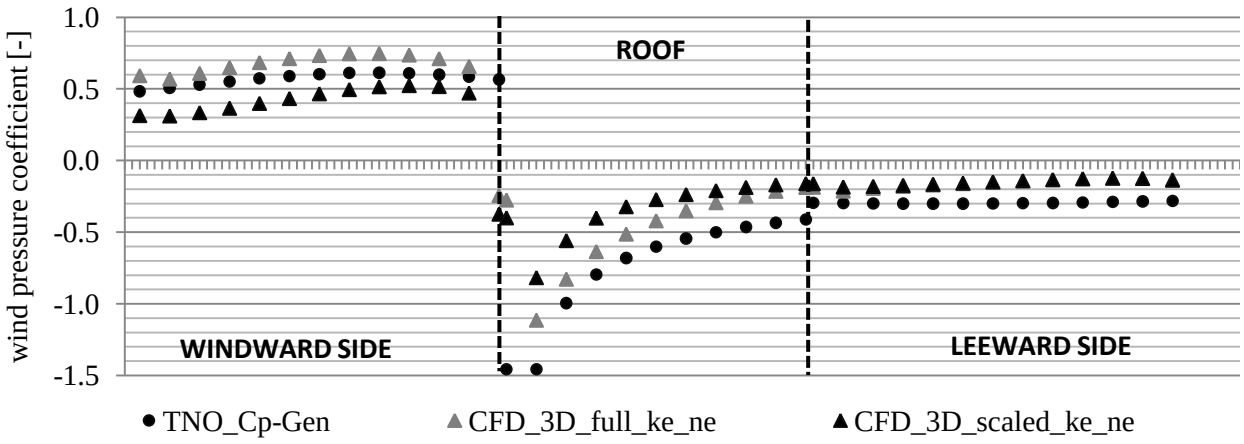

Fig. 2. Comparison of C_p-values between full scale and scaled model of closed building: verification with TNO C_p-Generator

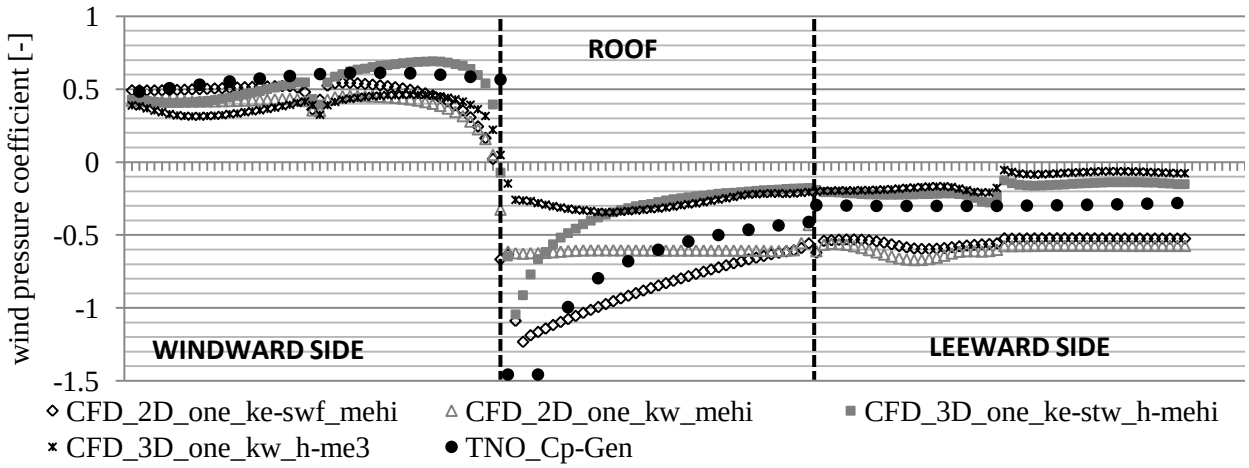

Fig. 3. Comparison of C_p-values: one opening (CFD), closed building (TNO)

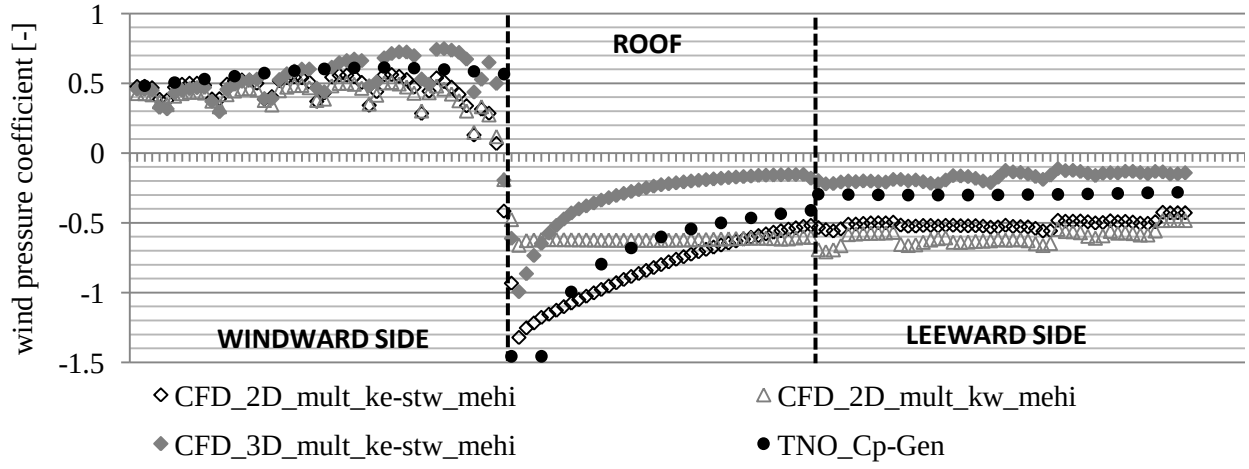

Fig. 4. Comparison of C_p-values: multiple openings (CFD), closed building (TNO)

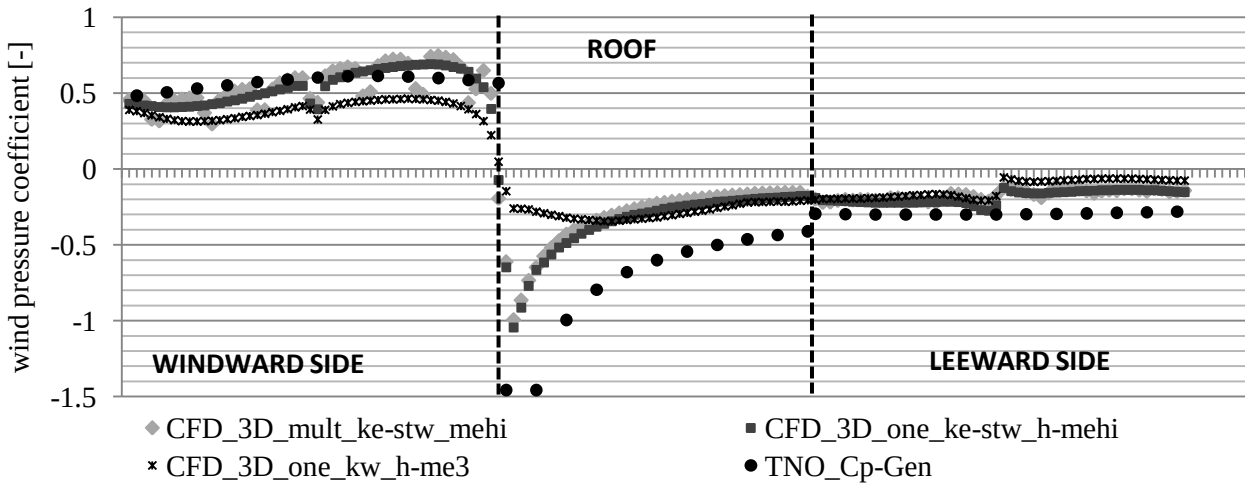

Fig. 5. Comparison of C_p-values: closed versus one or multiple openings (CFD_3D) and closed building (TNO)

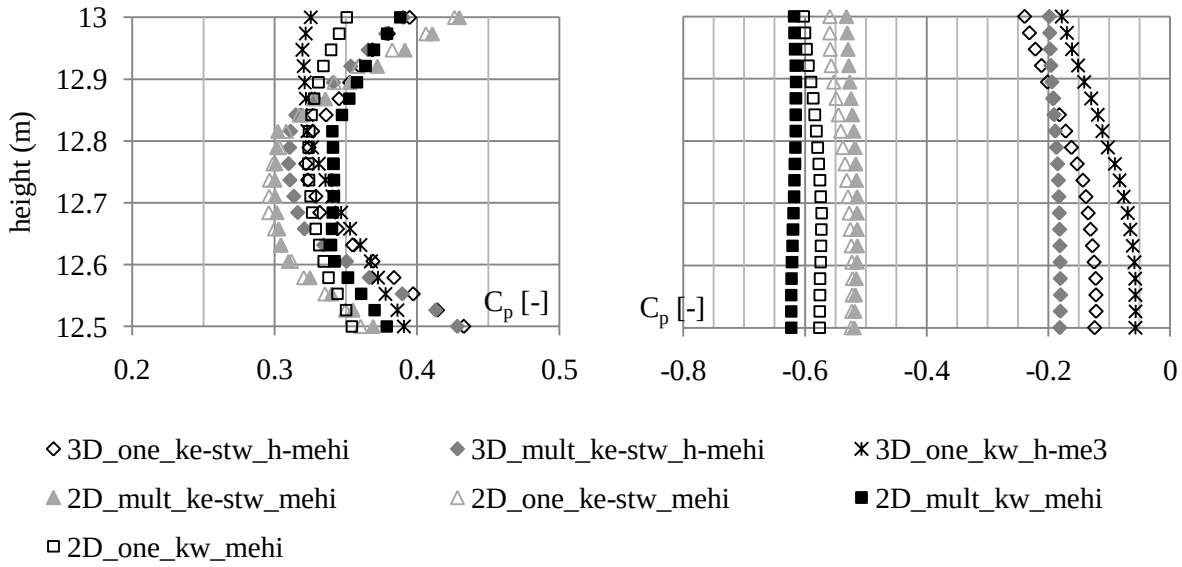

(a) FRONT – 20 cm from opening (b) BACK – 20 cm from opening

Fig. 6: Comparison of C_p-profile at opening

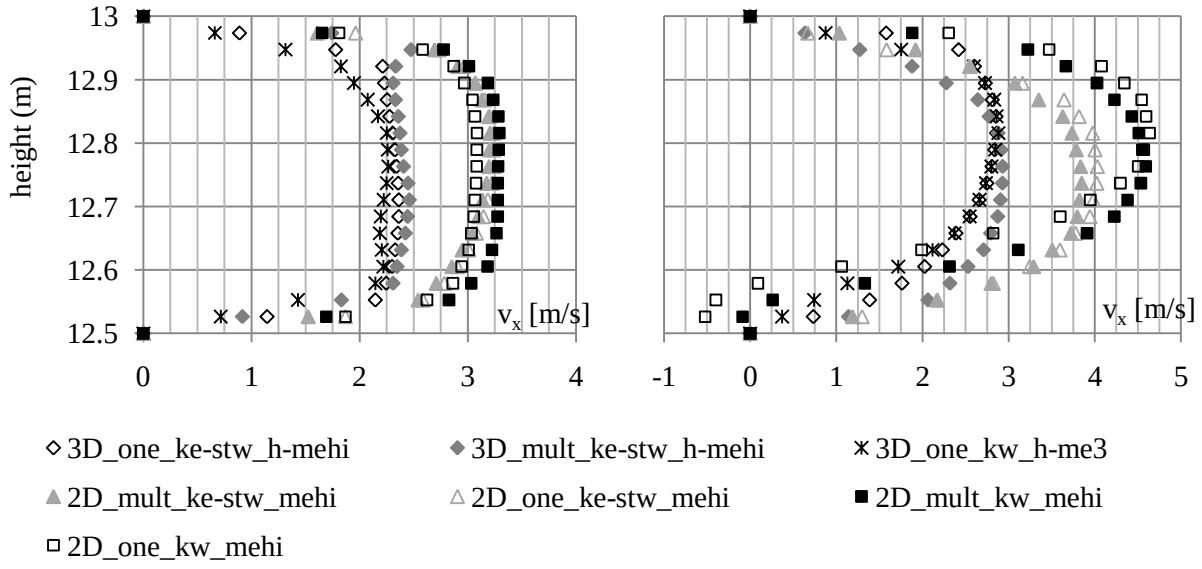

(a) FRONT – at opening (b) BACK – at opening

Fig. 7: Comparison of velocity profile at opening

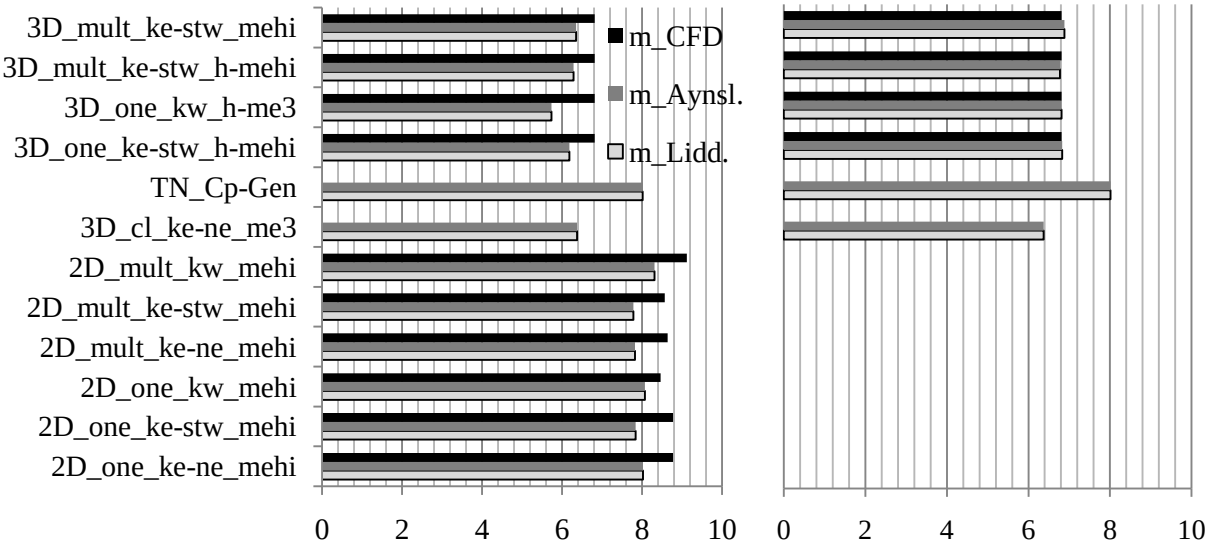

(a) fixed $C_d = 0.65$, $n = 0.5$ (b) adjusted C_d

Fig. 8: Comparison of resulting mass flow rates – according to CFD or to approximation formulas